Proceedings of the 4th World Congress on Civil, Structural, and Environmental Engineering (CSEE'19)
Rome, Italy – April, 2019
DOI: 10.11159/icgre19.1

Quantifying the Effect of Rolling Dynamic Compaction

Mark Jaksa[1], David Airey[2], Brendan Scott[1], Yien Lik Kuo[1], Tharanga Ranasinghe[1], Andrew Bradley[1], Oi Yin Chung[1], Yuxiao Li[2], Yue Chen[1]
[1]University of Adelaide
School of Civil, Environmental and Mining Engineering, Adelaide, Australia
mark.jaksa@adelaide.edu.au; brendan.scott@adelaide.edu.au; yien.kuo@adelaide.edu.au; tara.ranasinghe@gmail.com; andrew.bradley@adelaide.edu.au; oiyin.chung@adelaide.edu.au; yue.chen@adelaide.edu.au
[2]University of Sydney
School of Civil Engineering, Sydney, Australia
david.airey@sydney.edu.au; yuli2425@uni.sydney.edu.au

Abstract – Rolling dynamic compaction (RDC) is a ground improvement method that involves towing, typically with the aid of a tractor, a 3-, 4- or 5-sided, non-circular module. Due to the mechanics of its operation, as well as the increased travel speed of 10–12 km/h when compared with the 4 km/h speed of conventional vibrating and drum rollers, RDC has demonstrated improved earthworks efficiency and greater effectiveness at depth below the ground surface. Despite the significant benefits derived from RDC, much research is needed to facilitate the development of models to predict the extent of ground improvement, as a function of soil type, ground conditions, travel speed, module type and weight, and the number of passes. This paper presents the results of an extensive research program undertaken to quantify the behaviour of RDC and its consequent effect of the ground. The research involves field studies incorporating in situ measurement, laboratory testing of small-scale physical models involving novel instrumentation, numerical modelling using dynamic finite element analyses, and the implementation of artificial intelligence. Each of these aspects is treated in detail in the paper.

Keywords**:** Rolling dynamic compaction, Physical modelling, Finite element analysis, Discrete element modelling, Sensors.

1. Introduction

Developed in South Africa in the 1940s, primarily to improve collapsing soils [1], rolling dynamic compaction (RDC) has become successfully and increasingly utilised around the world in a wide range of applications, including civil construction works and large reclamation projects [2]; in the compaction of sites with non-engineered fill, such as industrial land or 'brownfield' sites; large highway rehabilitation [3]; in the agricultural sector to reduce water loss [4]; and in the mining sector to improve haul roads and tailings dams. RDC involves towing heavy (6–12 tonnes), non-circular (3-, 4- and 5-sided) modules, as shown in Fig. 1, which rotate about a corner and fall to impact the ground. RDC is becoming more popular because it is able to compact the ground more effectively, i.e. to greater depths than its static and vibrating roller counterparts, and more efficiently because of its greater speed; 12 km/h compared with 4 km/h using traditional rollers [5], and thicker lifts [6].

This paper presents an overview of recent research undertaken at the Universities of Adelaide and Sydney, Australia, to characterise the behaviour of RDC. In particular, the paper presents the results of field and numerical modelling of the 4-sided 'impact' roller (Fig. 1a) and laboratory testing of the 3-sided (Fig. 1b) and 4-sided modules. Advanced instrumentation and future work are also examined.

Fig. 1: Rolling dynamic compaction modules: (a) 4-sided (Broons); (b) 3-sided (Landpac); (c) 5-sided (Landpac).

2. Field Testing

Testing to verify the effectiveness of RDC in field applications typically involves undertaking pre- and post-testing to confirm if a project specification has been met. Verification techniques that have been used to assess RDC include intrusive techniques, such as dynamic cone penetration testing, cone penetrometer testing and field density testing. Non-intrusive techniques have also been adopted, including geophysical surveys, surface settlement monitoring and the use of a lightweight falling deflectometer. Due to space constraints, this paper will not discuss field testing methods in detail; however, a more comprehensive discussion, including factors that affect the choice of verification techniques for RDC applications, is given by [2], [7] and [8].

Intensive field trials have focussed on quantifying the change in stress imparted to the ground due to the 4-sided module using Geokon Model 3500 earth pressure cells (EPCs) [9]. The results presented here summarise the key findings from burying an EPC at a depth of 0.7 m in uniform fill material. Homogeneous fill comprising crushed rock, with a maximum particle size of 20 mm and produced at a local quarry, was used in lieu of natural soil to minimise the effects of soil variability, which can often conceal the true effects of RDC. The choice of sampling frequency is an important variable that needs to be considered. Avalle *et al.* [5] varied the sampling frequency between 200 Hz to 10,000 Hz and identified that a sampling frequency of at least 2,000 Hz was required to obtain sufficient data points to identify the peak pressure imparted to the ground. Fig. 2 shows the change in stress due to a single impact striking the ground, where a peak pressure of 873 kPa was recorded. A bespoke data acquisition system and LabVIEW software program [10] was used, whereby a sampling frequency of 4,000 Hz was adopted, resulting in one sample every 0.00025 seconds. The duration, Δt, over which pressure was imparted to the ground due to RDC was approximately 0.045 seconds, with approximately 180 data points defining the shape of the pressure impulse shown in Fig. 2.

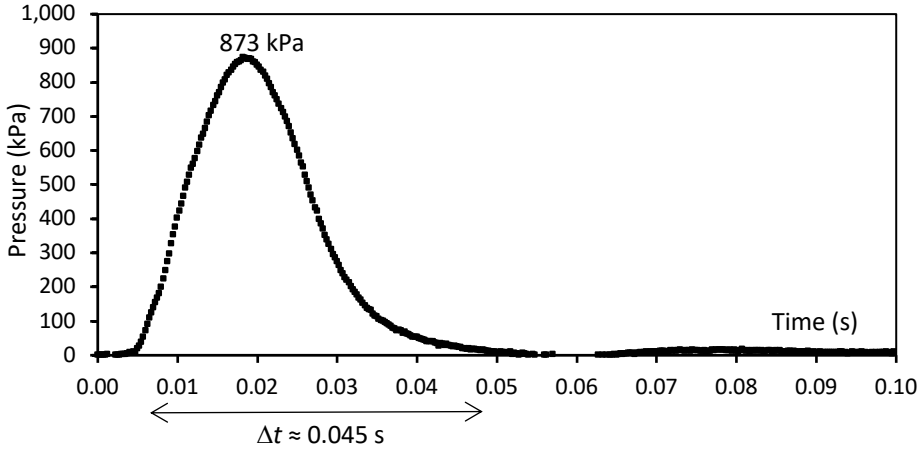

Fig. 2: Pressure change due to passing module at 0.7 m depth.

An important advantage of using EPCs is the ability to capture the module striking the ground in real-time which traditional pre- and post-compaction test methods are unable to achieve. A disadvantage of quantifying ground improvement using buried instrumentation at a fixed location is that the maximum pressure that is imparted to the ground will not be measured from every impact due to the asymmetrical geometry of the module. This is discussed in greater detail by [12]. EPCs have been used in conjunction with other verification techniques, to help quantify the depth of influence of RDC. Typical improvement depths of between 0.5 m to 3 m are common for RDC, depending upon soil conditions and a number of other parameters that are discussed in detail in [13].

Accelerometers have been used to quantify ground accelerations induced in the ground due to RDC. An accelerometer (± 16*g*) was also attached to the EPC buried at 0.7 m depth. As shown in Fig. 3, a peak downward (negative) acceleration of 13.2*g* was recorded before soil resistance could be mobilised, this was followed by an upward (positive) acceleration of magnitude 5.4*g*. The acceleration trace then dissipated back to 0*g* less than 0.1 seconds after the time of initial module impact.

A fast sampling rate is again required to capture ground accelerations; 4,000 Hz was used to obtain the vertical acceleration response shown in Fig. 3, whereby the downward acceleration occurred over a duration of roughly 0.01 seconds, with approximately 40 data points defining the negative accelerations that occurred due to the module striking the ground surface. Double integration of the acceleration-time response enables displacements to be evaluated provided that the accelerometers are stable. As the accelerometers were rigidly fixed to the EPCs, which were carefully buried in the ground, the resulting displacements are considered reliable. As shown in Fig. 4, a maximum displacement of approximately 7 mm was recorded less than 0.03 seconds after module impact; however, after unloading, a permanent displacement of approximately 4 mm was evaluated.

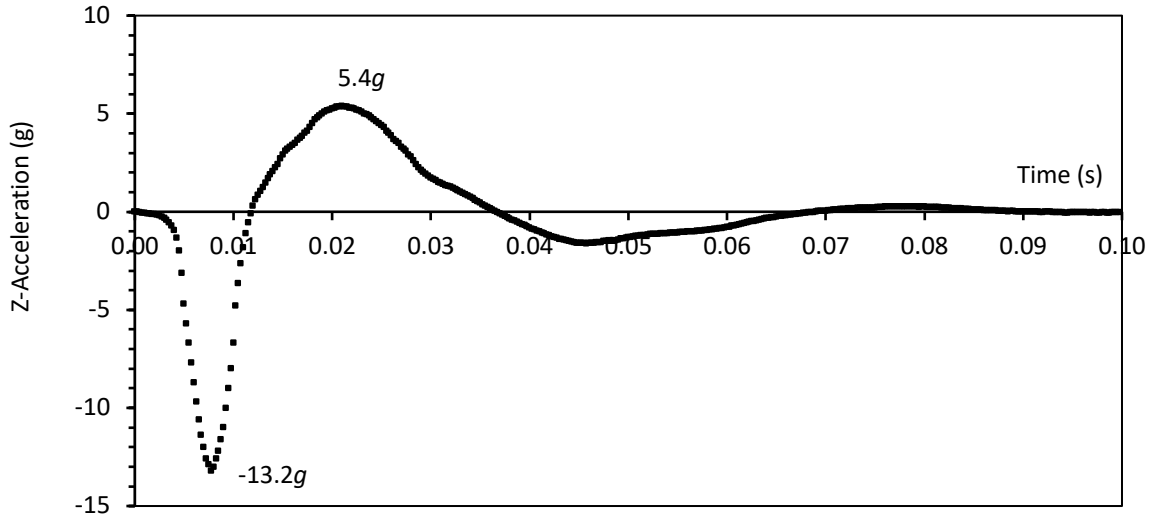

Fig. 3: Vertical acceleration response at time of module impact.

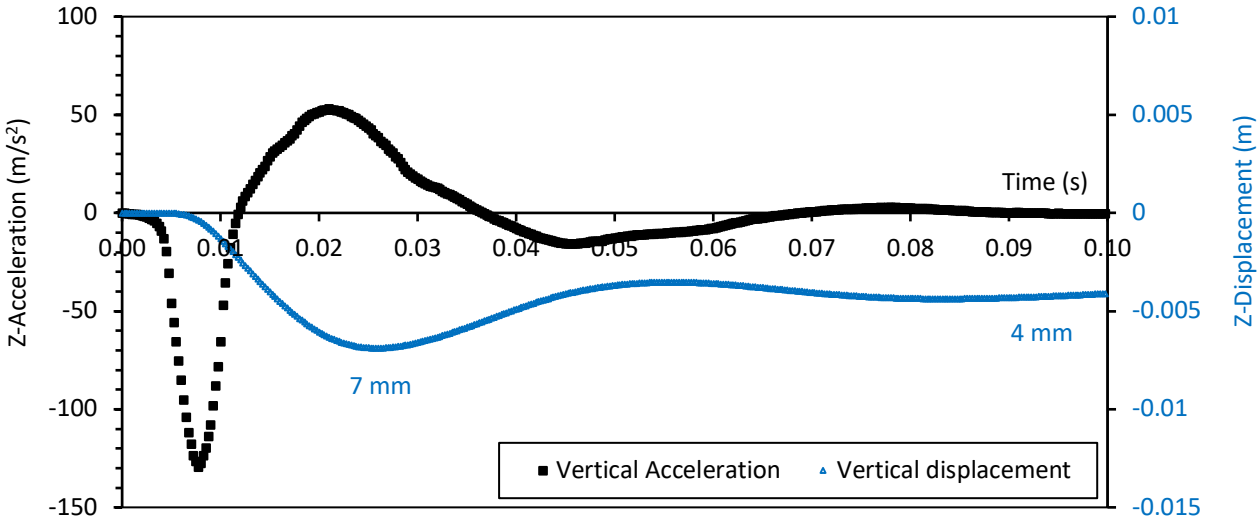

Fig. 4: Vertical acceleration and vertical displacement versus time.

Recent advances in instrumentation technology have enabled the dynamic effects of RDC to be more accurately captured than ever before. A greater understanding of soil response from field testing is an important step in being able to predict, with greater confidence, the performance of RDC in project applications. Additionally, field testing also enables calibration of computer simulations and physical scale modelling of RDC, which are discussed in later sections of this paper.

3. Laboratory Testing

A sophisticated scale model testing facility has been established to simulate RDC in a controlled laboratory environment, in order to understand and quantify the efficacy of RDC in a range of soil types and field conditions. Laboratory testing has been conducted on physical scale models of the 3- and 4- sided modules and these are discussed below.

3.1. 3-sided RDC Module

The Sydney University Pavement Testing Facility [14, 15] has been modified to enable testing of a model 3-sided RDC module. The facility consists of three main components, a test tank, an overhead track and a loading carriage. The support and guidance of the moving loading carriage is provided by an overhead rail. In the original configuration, shown in Figure 5a, the test wheel ran on a oval shaped wooden track when outside of the test section, and over a pavement in the straight test section. To avoid the wheel passing along the same track over the pavement section the test tank could be moved sideways by hydraulic actuators in a random, programmed manner. A conductor rail system supplies power to the motor which drives the wheel and hence the loading carriage assembly. Data acquisition only occurs as the wheel passes over the test tank and is controlled by micro switches at start and end points. Figure 5b shows the modified experimental configuration and Figure 5c detail of the module which was used to apply the rolling dynamic compaction. In the modified arrangement (Fig. 5b) the wheel is still used to drive the loading carriage, but it passes to the side of the test tank and, as it does this, goes over a ramp which has the effect of lowering the RDC module into the tank. The RDC module is spring loaded and has a maximum vertical displacement of 25 mm. When the wheel comes off the ramp it lifts the module clear of the track so that it only impacts in the test section. The test tank is 1.5 m long, 0.5 m wide and up to 0.6 m deep, although in tests described below the soil depth was limited to 270 mm by a false floor. The motor, which was connected to live rails, was used to power and control the speed of the wheel. In the tests described below a total of 25 cycles were used for a range of wheel velocities.

Since the apparatus was commissioned in 2014 by [16], different instrumentation has been used to investigate the soil displacements and the motion of the RDC module. The vertical and horizontal displacements within the soil have been measured using miniature (30 mm diameter) settlement plates that are connected to taut, lightly loaded, wires that pass through external LVDTs, installed at different positions within the box. The motion of the RDC module has been studied using wireless accelerometers mounted on the module and through tracking of patterns on the rotating module using high speed photography and digital image correlation (DIC).

Initial experiments using dry, uniform Sydney sand were unsuccessful because the RDC module pushed the loose, dry sand to the side and in front of it and little compaction occurred [16]. As a result, and because of the difficulty of

Fig. 5: University of Sydney test apparatus: (a) original pavement facility, (b) modified facility for RDC testing, (c) details of 1:20 scale model.

compacting dry sand in practice, it was decided to use well-graded river sand and to add additional fines to suit the scale of the experiment setup. The well-graded sand was mixed with 20% non-plastic fines. Although the RDC module effectively compacted this material, there was still a significant amount of soil pushed out of the way. In practice, when dealing with very loose sands, a working platform typically 300 mm thick is placed on the soil surface to enable the tractor to traverse the site and to prevent bogging of the RDC module. Ideally a scaled working platform of dense material would be used, but because of the small scale, approximately 1:20, any working platform soil layer would need to be very thin and thus difficult to prepare and in addition would contaminate the test material affecting test repeatability. Experiments were performed by [17] to establish a suitable material to act as a working platform. Various thin fabric and plastic materials were tested. It was found that a 3-mm thick rubber sheet gave the best performance in terms of its ability to ensure effective transfer of energy from the RDC module to the soil and gave the greatest surface soil settlements and depth of compaction.

Results are presented in Figure 6a to show the vertical settlements after 25 passes for a series of tests performed with different RDC module velocities. The soil used in the experiments was a silty gravelly sand that was considered to have a grading typical of many materials used as fills in construction projects and to be typical of loose soils that need to be compacted more generally. The tank was emptied and re-filled between each test in order to maintain an initially similar, relatively loose, soil density. Figure 6b shows the surface in a typical test after 25 passes, indicating the effectiveness of the compaction.

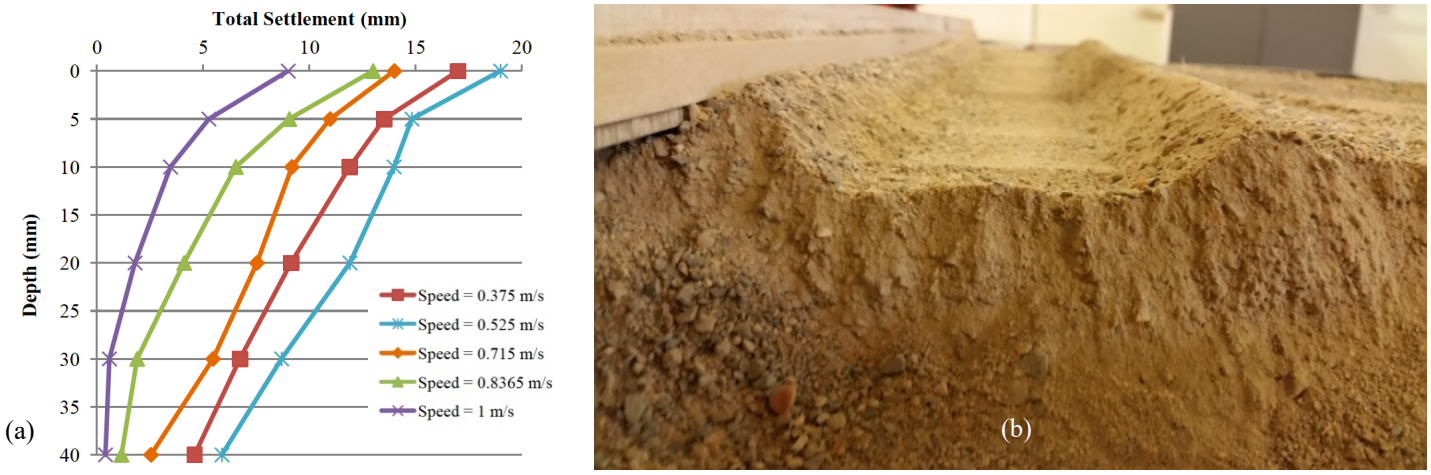

Fig. 6: Typical test results: (a) vertical displacement profiles after compaction at different module speeds, (b) compacted soil surface.

The vertical deformations profiles show as expected that the settlement decreases with depth. In addition, it is observed that the maximum measured settlement occurs at a maximum linear velocity of 0.525 m/s, which represents about 6 impacts per second. As the energy transmitted to the ground is expected to increase with velocity and magnitude of the impact the increase of settlement is expected. However, in practice, higher speed operation is difficult because of vibrations transmitted to the tractor, a tendency for the compactor modules to bounce over the ground and there are practical limitations such as wear and tear of machine parts, fuel consumption and emissions which also influence the choice of travelling speed [18]. Avalle [19] suggests that at high travel speeds, the time is not sufficient for the load to be effectively applied to the underlying soil, which is supported by the results from these model tests. In practice, typical tractor velocities of around 3 m/s are used, which correspond to approximately 2 blows per second. As the model tests indicate, optimal compaction occurs at about 6 blows per second, there may be benefit in travelling at higher speeds at field scale if machine limitations can be overcome. However, more research is required to confirm the trends and the optimum speed and to explore this further a new larger scale model has been developed to investigate scale effects. The results shown in Figure 6 also indicate that the RDC process induced vertical strains ranging from 14.3% to 28.6% in the soil. This is in agreement with field test results which show that RDC can induce vertical strains of up to 30% in similar soil types [19, 20]. This suggests that the scaled model is capable of providing results which are reasonably representative of the actual field-scale behaviour of soil under rolling dynamic compaction.

3.2. 4-sided RDC Module

The Broons-University of Adelaide facility, located at Gillman, South Australia, incorporates a test rig (Fig. 7), which consists of an elliptical track and two 1.2 m high × 0.75 m wide × 1.075 m long steel bins, containing the soil to be improved by the RDC model and incorporating embedded instrumentation. A 1:13 RDC scale model (Fig. 6) is towed along the track by a chain-driven carriage, which is powered by a variable-speed, electric motor. Two physical models of the 4-sided RDC module have been investigated to date using the testing facility. Both models have identical dimensions (115 × 115 × 100 mm) and weigh 3.64 and 5.46 kg and are, respectively, 1:13 scaled replicas of the Broons' 4-sided BH-1300 (8-tonne) and BH-1300 HD (12-tonne) impact rollers.

Fig. 7: Test facility at Gillman, South Australia.

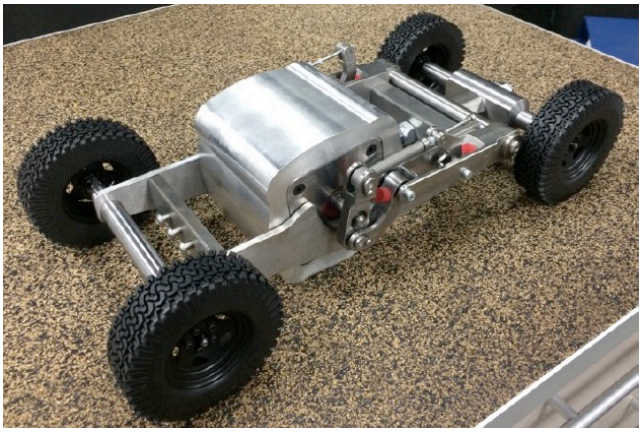

Fig. 8: 1:13 replica of Broons BH-1300 4-sided impact roller.

In order to investigate the efficiency of RDC in different soil types typically encountered in civil construction projects globally, the testing program includes a range of soil types. Granular soils have been studied, thus far, including (1) a readily available and homogeneous Sandy Gravel sourced from Monarto Quarries, South Australia, (2) Sandy Loam that contains uniform fine sand with less than 20% silt and clay; and (3) a poorly-graded coarse-to-fine Sand with a trace of silt. A series of soil classification and consolidation tests have been performed to determine the basic soil characteristics of the soil and the results are summarised in Table 1. The other soils that will be considered in the future include clayey sand, sandy clay, and clay (low and high plasticity).

Chung *et al.* [21] presented the test results of a 1*g* 1:13 scale model of the scale model of the 8-tonne Broons BH-1300 module, using Sandy Gravel. The model traversed along a track at a speed of two-impacts per second, which is equivalent to prototype speed of 12 km/h and compacted the soil inside the soil bins up to a total of 80 passes. As the first step in the model testing, the soil was weighed and then thoroughly moisture conditioned prior to placement in the

Table 1: Soil characteristics for RDC model compaction testing.

Soil property	Soil type		
	Sandy Gravel	Sandy Loam	Sand
UCSC classification and soil description	GW, fine to medium gravels with some sand	SP, poorly graded fine sand with some silt and clay	SP, poorly graded coarse-to-fine sand with trace of silt
Specific gravity	2.62	2.62	2.60
Standard optimum moisture content	12%	11%	13%
Initial soil density for testing	14.2 kN/m^3	15 kN/m^3	15 kN/m^3
Initial void ratio of soil e_0	0.87	0.71	0.70
Standard maximum dry density	19 kN/m^3	18.7 kN/m^3	18.2 kN/m^3

soil bins to achieve a consistent moisture content of 12%. The soil was weighed and placed into the bins in layers of approximately 100 mm in thickness in order to achieve a uniform initial density. During the process of placing the soil in layers, Keller Series 9 PD earth pressure cells (EPCs), 19 mm diameter piezo-resistive pressure transducers, were embedded in depths between 50 and 300 mm below the soil surface. The results of the experiments showed that the magnitude of measured stress changes reduced with increasing depth, as one would expect, and relatively low readings were recorded at depths below 200 mm. Figure 9 presents the peak soil pressures predicted at different depths if compacted using a prototype in the same soil and compared with results of full-size RDC field studies [12]. Chung *et al.* [21] also predicted that the depth of improvement is approximately 2 m for the Sandy Gravel tested, which is in general agreement with the field test results of [12], who tested the same soil in field trials using a full-size BH-1300 impact roller.

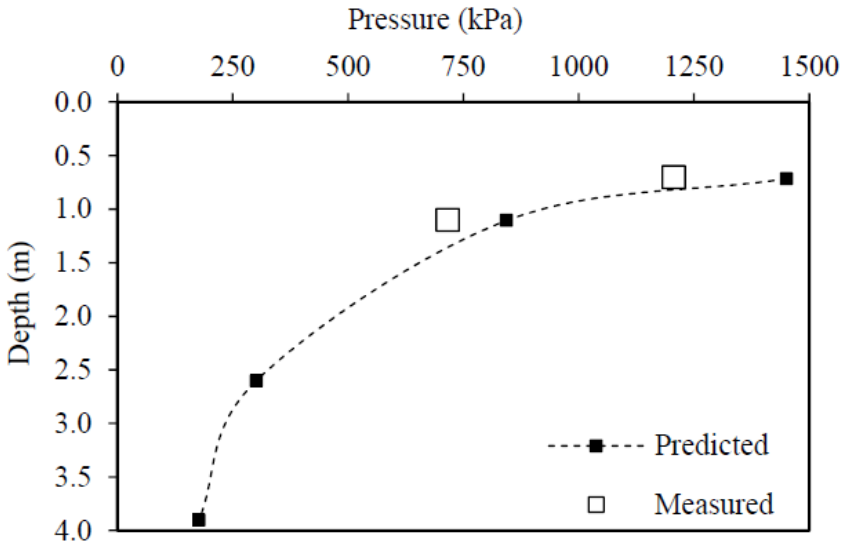

Fig. 9: Predicted pressures from model compaction versus measured pressures from full-size module [21].

Using Sandy Loam and Sand, the 1:13 models of the 8-tonne BH-1300 and 12-tonne BH-1300 HD modules have been investigated, for the the effects of compaction with respect to the travel speed of the RDC modules. A total of 120 RDC passes were conducted for each test. Each model traversed the soil surface at speeds of 0.256, 0.299 and 0.363 m/s, which represent prototype speeds of 12, 14 and 17 km/h, respectively, based on the 1:13 scaling ratio in the linear dimension. Fifteen sensors were embedded in the soil bin, of which 9 were aligned along the centreline of the direction of traverse of the model compactor in order to capture the peak dynamic pressures. To provide data for assessing the extent of compaction in the lateral direction, the remaining 6 sensors were placed at distances of 100 to 200 mm offset from the centreline. Each sensor is equipped with a miniature EPC, which consists of a 19 mm diameter Keller Series 9 PD piezo-resistive pressure transducer, and tri-axial accelerometers in the X, Y and Z directions, for the purposes of measuring the vertical and lateral accelerations and tilt. Using a bespoke data acquisition system and the commercially-available LabVIEW software program (see www.ni.com/en-au/shop/labview.html), the responses of the EPCs and accelerometers were recorded using a sampling frequency of 2 kHz. The surface settlement of soil due to RDC compaction have been measured using a hand-held 3D scanner, as discussed below.

4. Advanced Laboratory-based Instrumentation

This section examines advanced instrumentation technologies that have to date been adopted at the Broons-University of Adelaide facility to assist with understanding better the characteristics of RDC. These include pressure mapping sensors and 3D surface scanning.

4.1. Pressure Mapping Sensors

Accurate determination of peak stresses and stress distributions in geomaterials are critical to accessing the efficacy of RDC. As discussed above, buried load cells, also known as earth pressure cells, EPCs, are commonly used to measure stresses in soils, and a bespoke EPC design has been adopted in the present research study, as discussed above. The EPC is specifically designed to be stiff and cylindrical in shape and to have a minimum height-to-diameter ratio, such that it has as minimal impact on the stress distribution as possible. The EPC usually incorporates a rigid outer rim to mitigate local stress concentration effects. As described above, such EPCs have been used in RDC research to estimate the peak stress, as well as the variation in stress with time in the soil mass. To obtain a spatial variation of the stress field, a number of EPCs can be deployed in close proximity to one another over an area of interest. However, this method will introduce uncertainties and inaccuracies due to soil arching and stress shadowing effects.

An alternative is to employ tactile sensing technology that was originally developed at the Massachusetts Institute of Technology [22, 23] and is available by Tekscan (www.tekscan.com). The tactile pressure sensors represent a relatively new technology, which make use of a thin (0.1 to 0.3 mm thick), flexible, grid-based, tactile pressure sensors for measurement of pressure fields, particularly in granular materials. These tactile sensors incorporate a grid of force sensing cells (known as sensels) which facilitate pressure measurements in high-resolution.

A standard tactile pressure sensor is typically comprised of a regular grid of conductive materials that is printed on two polymeric sheets (Fig. 10a). Between this grid of conductive materials is a second layer consisting of a grid of force-sensitive semi-conductive ink. These two grids are sandwiched between two polymeric sheets. The intersections of these grids form sensing areas. When pressure is applied, the electrical resistance of the semi-conductive material changes. The tactile sensors are connected to 'handles' (Fig. 1c) and a data acquisition (DAQ) board. The DAQ board scans the sensels and records the electrical resistance at each intersection. Calibration is required to relate the electrical resistance to the externally applied force/pressure and is performed using manufacturer-supplied software [24]. It is suggested that the calibration of sensors be performed under similar conditions to the application, including applied pressure, interface material and duration of loading [24]. In the case of RDC, the duration of loading is very short, i.e. around 45 ms. Dropping a known mass from a known height and measuring the peak deceleration is the preferred method for calibrating these sensors. In order to facilitate this, at University of Adelaide, a standard Proctor compaction hammer was fitted with a 200*g* accelerometer (Fig. 11).

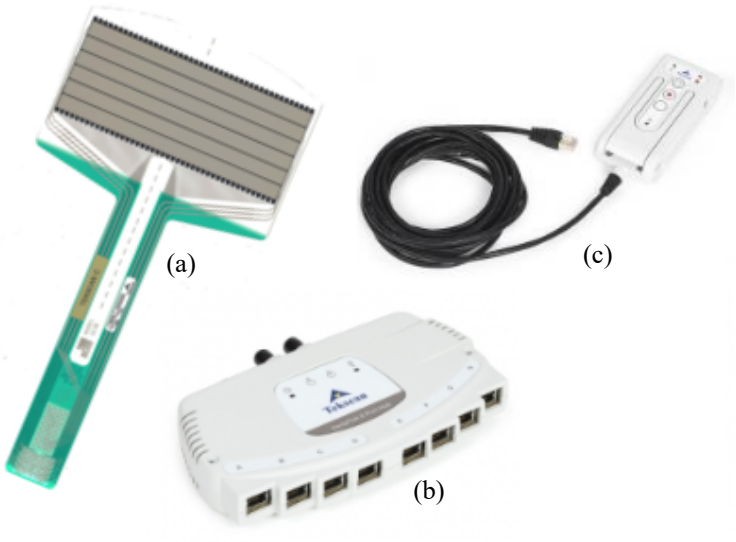

Fig. 10: Tactile pressure sensing equipment: (a) Tekscan sensor model 5570; (b) 8-port VersaTek hub; (c) VersaTek handle.

Fig. 11: Sensor calibration using an instrumented Proctor compaction hammer.

Tactile pressure sensors have been used in a wide variety of engineering and medical applications and they have also been adopted by several geotechnical engineering researchers [25-28]. The Tekscan pressure sensors are well suited for physical modelling of RDC. After careful consideration, the sensor model 5570 was selected (Fig. 1a). This particular model has 264 sensels arranged in a matrix, with each measuring 82.3 × 212.3 mm, which translates to 1.5 sensels for every square centimetre. This particular sensor model is capable of providing data at a high sampling rate – up to 4,600 frames per second, which makes it suitable for capturing the dynamic loading induced by RDC. Figure 12a shows a typical stress distribution map, produced by the Tekscan sensor and associated software, and Figure 12b presents a typical force versus time plot.

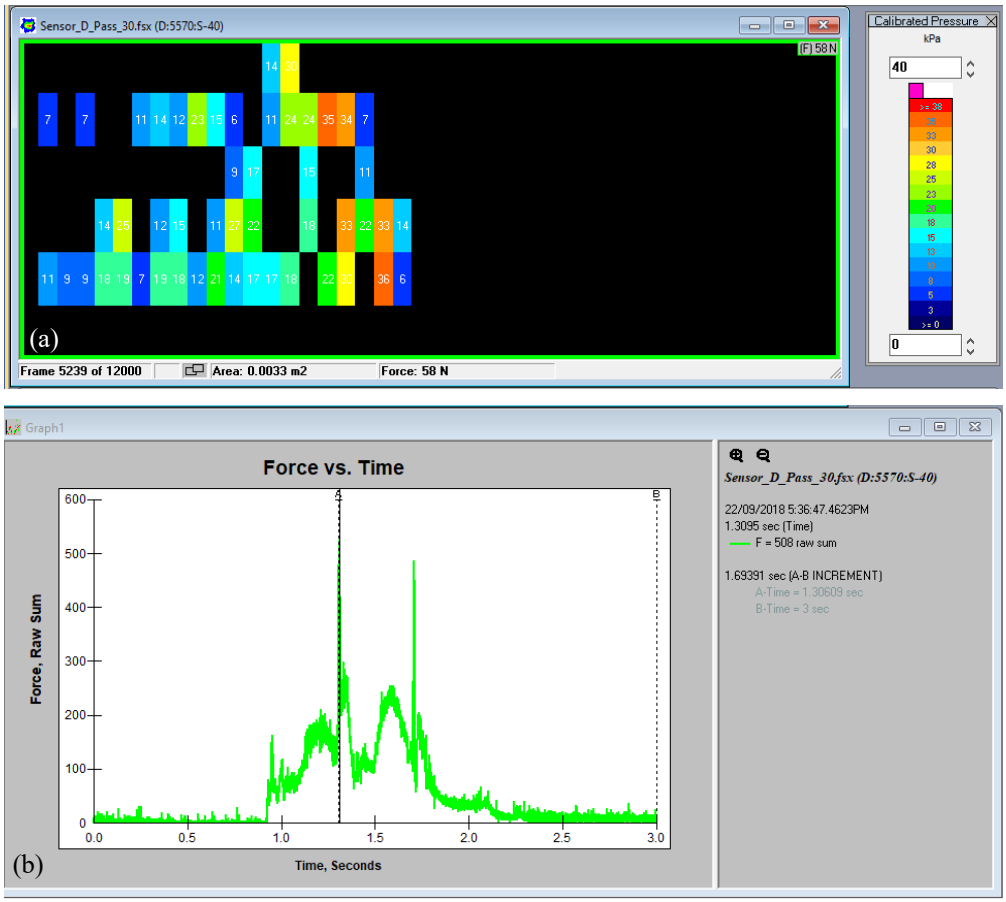

Fig. 12: Typical tactile pressure sensor results: (a) stress distribution map, (b) force versus time plot.

4.2. 3D Scanning

Ground settlement provides an indirect assessment, but nonetheless an effective method, for quantifying the efficacy of RDC. Such an approach is a standard part of RDC field testing [7]. As occurs in the field, the scaled RDC module produces non-uniform undulating ground surface profiles. To determine accurately the average ground settlement with respect to the number of RDC passes, reasonably high-density measurements of the ground surface are needed. Manual methods would be inefficient and inaccurate. Recently, the University of Adelaide has adopted a high-precision 3D scanner technology (*EinScan Pro+* [29]) which involves no physical contact with the ground surface. This particular scanner uses non-laser, white light as the light source to generate a highly accurate (± 0.05 to 0.3 mm) 'point cloud' from the surface of an object in a very efficient manner (550,000 point per second) [29]. It can make use of features, such as the contours of a surface or adhesive reflective markers, as points of reference for alignment, and it is able to capture fine details in high-resolution (points are 0.2 to 3 mm apart in the point cloud). An example of a typical point cloud captured during a model test is shown in Figure 13 and the variations of ground settlement, with respect to the number of passes, are presented in Figure 14.

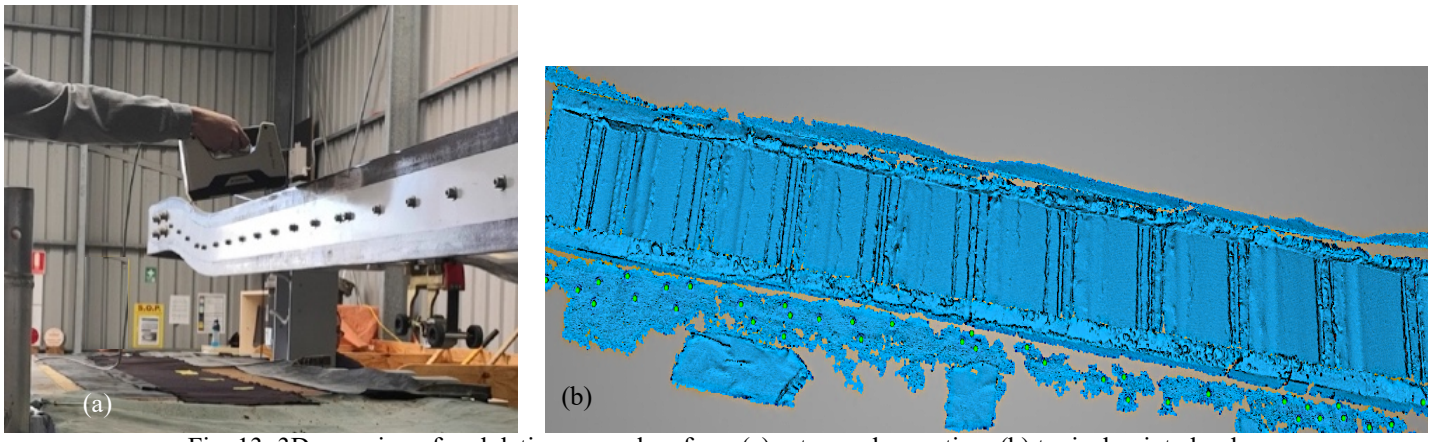

Fig. 13: 3D scanning of undulating ground surface: (a) setup and operation, (b) typical point cloud.

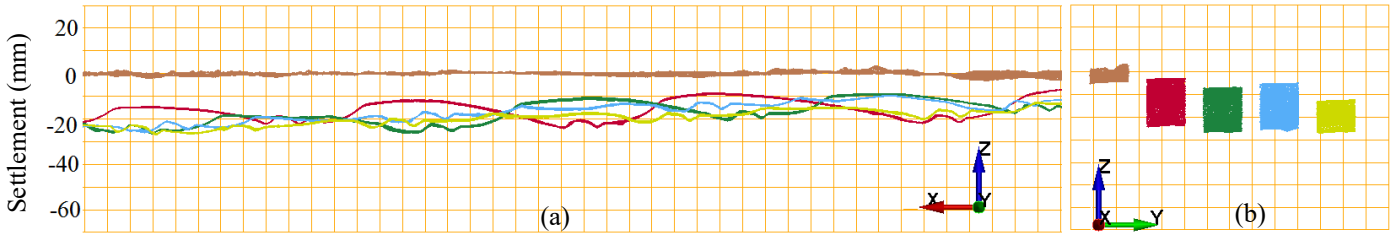

Fig. 14: Elevation views of surface settlement (mm): (a) front, (b) side.
(Legend: No. of passes: 0: brown; 10: red; 20: green; 30: blue; 40: gold.)

5. Finite Element Modelling

Numerical modelling, utilising the finite element method (FEM), has been undertaken to model the ground improvement as a consequence of RDC using the 4-sided roller and the 3-sided module. The former adopts the dynamic finite element analysis (FEA) software LS-DYNA (www.lstc.com/products/ls-dyna), whereas the latter adopts ABAQUS (www.3ds.com/products-services/simulia/products/abaqus/). Each are discussed in turn below.

5.1. Analysis of the 4-sided Roller

Although the accuracy of the FEA associated with the 4-sided roller has yet to be fully validated against field test results, the FEM is generally considered to be an appropriate investigative tool. It is suggested that, by applying a dynamic transient, non-linear model, a detailed analysis may be conducted in conjunction with field investigations to provide a greater understanding of the mechanics of RDC.

Past efforts to quantify the effectiveness of RDC by adopting the FEM [30–34] have the common limitation of tending to rely on typical or assumed values, as opposed to conducting bespoke field and laboratory studies. Importantly, their assumptions are inclusive of the kinematics, or motion, of the module. By adopting an assumed and constant motion of the module, typically based on approximations, the interaction between the soil and module are, more or less, pre-determined and may not necessarily represent the true behaviour.

Apart from a highly idealised study by Clifford and Bowes [35], there is no prior study that has explicitly examined the kinematics of the 4-sided roller. Hence, it is understandable that assumptions have been made in the aforementioned numerical investigations, due to the absence of information.

5.1.1. Motion of the 4-sided Roller

A study was conducted to investigate the kinematics of the 4-sided roller, during typical operation over a controlled field trial, in order to prescribe the motion of the module within a FEM framework. A field trial was undertaken utilising the BH-1300, 8-tonne, 4-sided impact roller. In brief, a 12 × 7.5 m test pit was excavated to a depth of 1.5 m and

backfilled with a local, well-graded sandy gravel fill material. High speed photography of the roller was carried out using a digital video camera, capturing 1,000 frames per second at a resolution of 1,280 × 1,024 pixels. The motion of the roller was recorded under typical operating conditions for the compaction of a controlled fill material, which involves being drawn behind a tractor travelling at a speed of 10 km/h performing 30 passes. From the video footage, time histories of the vertical (V_y), horizontal (V_x) and angular (ω_x) module velocities were calculated for each of the passes.

As it was observed that there was no clear dependence of the motion of the module with respect to the number of passes, a typical kinematic profile, relevant to all 30 passes, is investigated. This is undertaken to simplify the results into a single trend that can then be entered as the prescribed motion within the FEM. This is achieved by adopting a zero lag, 4th order Butterworth low pass filter, as shown in Figure 15 (positive velocity is downward). Moreover, by determining the period of impact (A-B) to be wholly representative of the period when the energy of the roller is transferred to the underlying soil, the average magnitude of energy imparted for compaction purposes may be quantified and verified within a FEM framework.

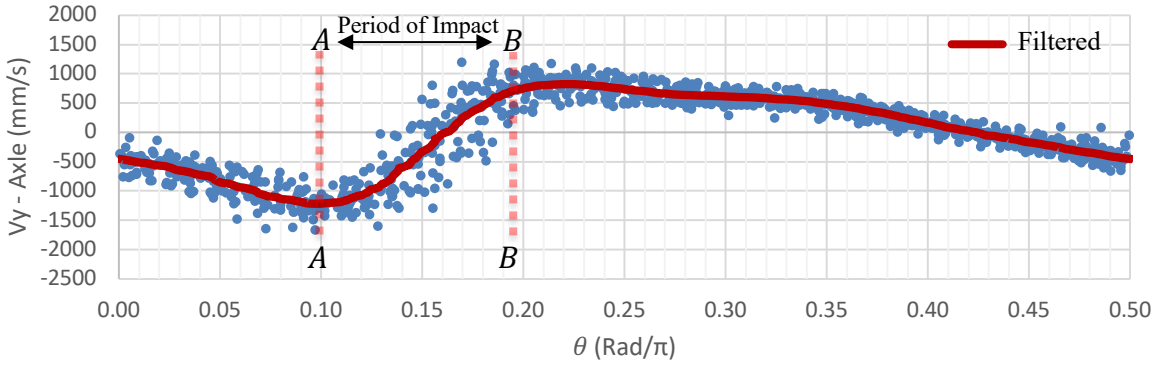

Figure 15: Low pass filtered vertical velocity – period of 0.5. (Positive velocity is downward.)

5.1.2. Finite Element Model of the 4-sided Roller

A number of FEMs are constructed in the commercial FEM software, LS-DYNA (www.lstc.com/products/ls-dyna), similar to that described by Bradley *et al.* [36] and Kuo *et al.* [33], albeit with some modifications. The sandy gravel is represented by a single-layered, homogeneous, soil mass constructed using quadrilateral elements, with either the default constant stress solid element (ELFORM 1), or the fully integrated, selectively reduced, solid element formulation within LS-DYNA (ELFORM 2). The dimensions of the elements in the domain of interest are specified as 200 × 200 × 200 mm^3 at the largest, and 100 × 100 × 100 mm^3 at the smallest. The global soil body dimensions are set to be 24 m long × 19 m wide × 4.6 m high, as shown in Figure 16. Non-reflecting boundary conditions are invoked (using LS-DYNA's *BOUNDARY_NON_REFLECTING keyword) to simulate infinite boundary conditions. The soil body is constituted using the Mat_014 (*MAT_SOIL_AND_FOAM_FAILURE) model provided within LS-DYNA. Although alternative material models have been investigated, Mat014 has been found to be reasonably reliable. The soil parameters were defined from laboratory- and field-based estimates, in conjunction with some assumed values that are typical for a sandy gravel.

In a manner similar to that undertaken by [36] and [37], material Rayleigh damping 5% of critical, at 0.01 and 100 Hz for the lower and upper reference frequencies, is defined for the soil body to represent the internal material damping commonly observed in the dynamic behaviour of soils. Additionally, to reduce the risk of the numerical phenomenon of element locking, where the displacement is underestimated under particular conditions, an hourglass control option, using Belytschko-Binderman's [38] formulation, may be utilised.

To initialise the model, *CONTROL_DYNAMIC_RELAXATION is utilised to implement gravitational loading and the settlement of an initially homogenous soil body to reach a representative in-situ profile. Whilst the soil deforms, the modules' relative height above the soil is maintained to reflect h_{Roller}, with an initial orientation reflecting $\theta = 0$.

Provided the accurate initialisation of the soil and roller at the conclusion of LS-DYNA's dynamic relaxation phase, the dynamic transient phase begins. LS-DYNA's keyword, *BOUNDARY_PRESCRIBED_MOTION_RIGID, is used to constrain the motion of the roller to that of the $\widehat{V_y}$, $\widehat{V_x}$ and $\widehat{\omega_x}$ time histories for successive impacts. A semi-constrained

condition, whereby the vertical velocity is relaxed, is also examinable for comparison purposes; where the vertical component of the module is unconstrained to allow the model to calculate the roller's vertical behaviour. Ideally, the model should reproduce a similar vertical velocity profile to that observed from the field. In order to undertake multiple passes, the roller is lifted up, the rotation paused, and the module brought back some distance (varies between each pass) and then carefully and slowly placed down on to the soil to continue its aforementioned prescribed motion.

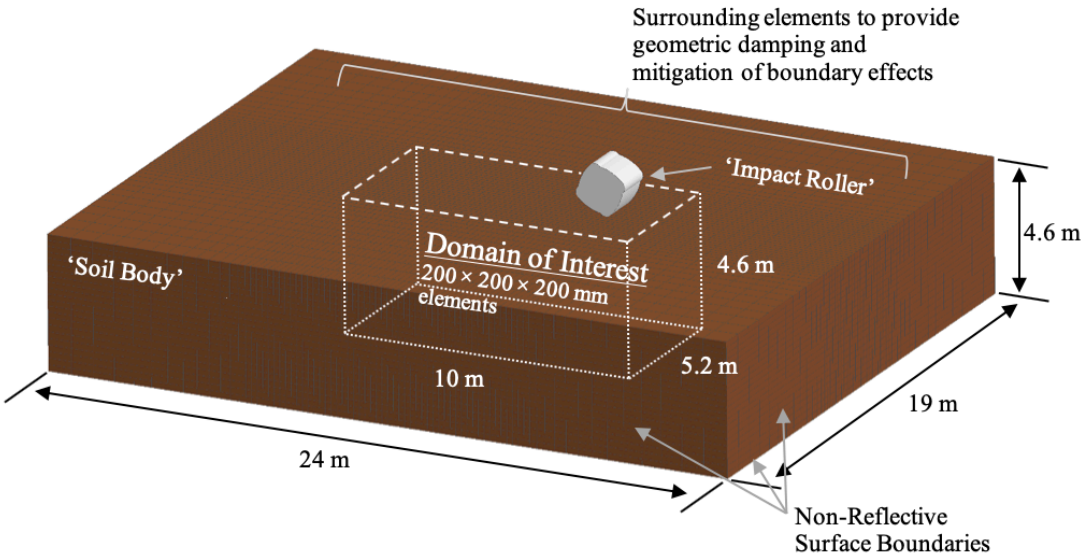

Figure 16: Global LS-DYNA model layout.

5.1.3. Results of Finite Element Analyses of the 4-sided Roller

A key benefit of the FEM is the ability to review the behaviour of the soil as the roller traverses the ground surface. This includes, but is not limited to, the stress distribution and the densification of the soil as a consequence of RDC, two examples of which are shown in Figure 17, with Fig. 17a showing vertical stress contours and Fig. 17b volumetric strain contours, both decreasing with depth.

It has been observed that the numerical model results align reasonably well with field test measurements. For example, the semi-constrained roller motion configuration is shown to be relatively consistent with both the fully constrained roller motion and that observed in the field, as shown in Figure 18. The model's predictions of $\widehat{V}_y$ suggest that an accurate account of the roller's kinematic motion has been obtained, noting that the vertical velocity trends towards that observed in the field.

5.2. Finite Element Analysis of the 3-sided Module

At the University of Sydney, the finite element software ABAQUS (www.3ds.com/products-services/simulia/products/abaqus/) is being used, in conjunction with the scale model laboratory tests, to model the 3-sided module. As with the 4-sided module analyses described above, the ABAQUS model consists of two parts: the 3-sided module and the soil body. The Drucker-Prager constitutive model is adopted for the soil body and a rigid body constraint is applied to the module. The results from the simulation are compared against the experimental measurements of [39] and [40].

Figure 19 shows soil settlement at different depths from both the experiments conducted by [40] and early results from the ABAQUS simulations. As can be observed, there is a significant difference between the two sets of results. There are two possible reasons for this. Firstly, the soil used by [40] was a mixture of river sand and feldspar, which results in the geotechnical properties being different to the pure sand adopted in the numerical model. In addition, the duration of the impact loading in the field, as discussed above is very fast, 0.045 s for the 4-sided roller, which is much faster than that adopted in the simulation.

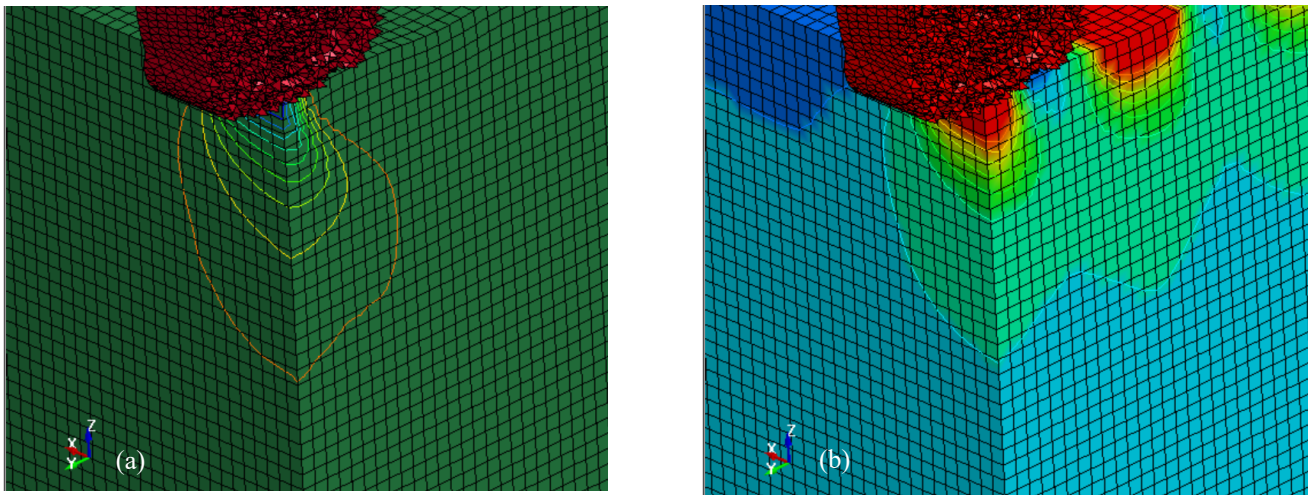

Figure 17: Typical LS-DYNA results: (a) pressure distribution, (b) volumetric soil strain after one RDC pass (4-sided module).

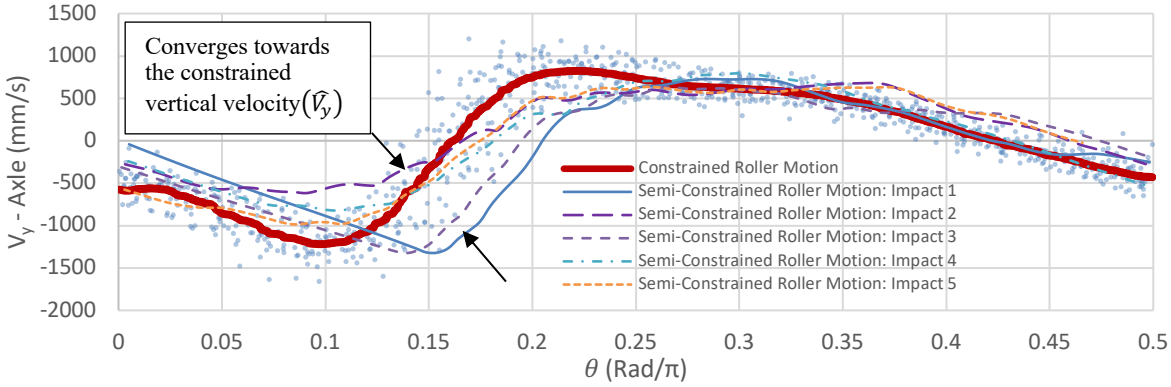

Figure 18: Comparison of the constrained vertical velocity $(\hat{V}_y)$ and that calculated from the semi-constrained model (4-sided module). (Positive velocity is downward.)

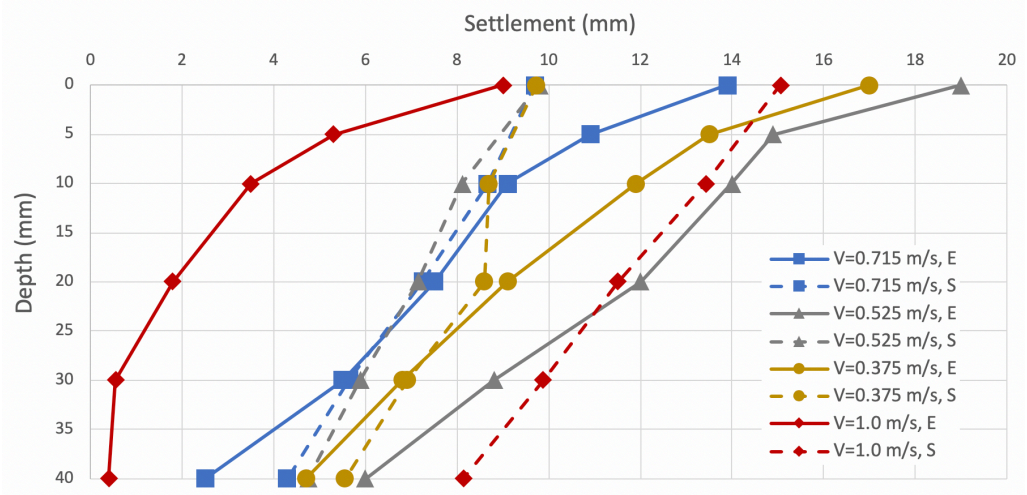

Figure 19: Comparison between measured and numerically predicted settlements (3-sided module). (Legend: E = experimental, S = simulation)

The surface settlement results, from the experiments by [39] and the preliminary simulations, are plotted in Figure 20a. As can be seen, the experimental surface settlements, from the first pass onwards, are much greater than those predicted by the simulation. In practice, the elastic modulus is influenced by the confining pressure and thus, in the experiments, the soil modulus near the ground surface was close to zero. However, in the simulation, the elastic modulus was set to a constant value of 15 MPa. Furthermore, in the experiments, as mentioned above, a significant amount of soil was pushed to the side of the module's path. These two factors contribute greatly to the difference. It is, however, pleasing that after the first pass, the two curves become almost parallel.

The stress distribution results are presented in Figure 20b. The curves show the results from the simulation, while the points represent the experimental results. At a depth of 5 mm below the surface, the stresses obtained from the simulation are greater than those from the experiments. However, at depths of 15 mm and 25 mm, the stresses obtained from the simulation are smaller than the experimental results. This can also be explained by the modulus of the soil near the surface. As mentioned above, the soil near the surface is much stiffer in the simulation than in the experiments, and this results in larger stresses. However, in general, the trend of the stress distribution shown by the curves is similar to that shown by the experimental data. Moreover, the stresses after the 5th, 10th and 15th passes, were greater than the stresses after the first pass, which represents densification of the soil. It is important to stress that the results presented are preliminary and research is continuing.

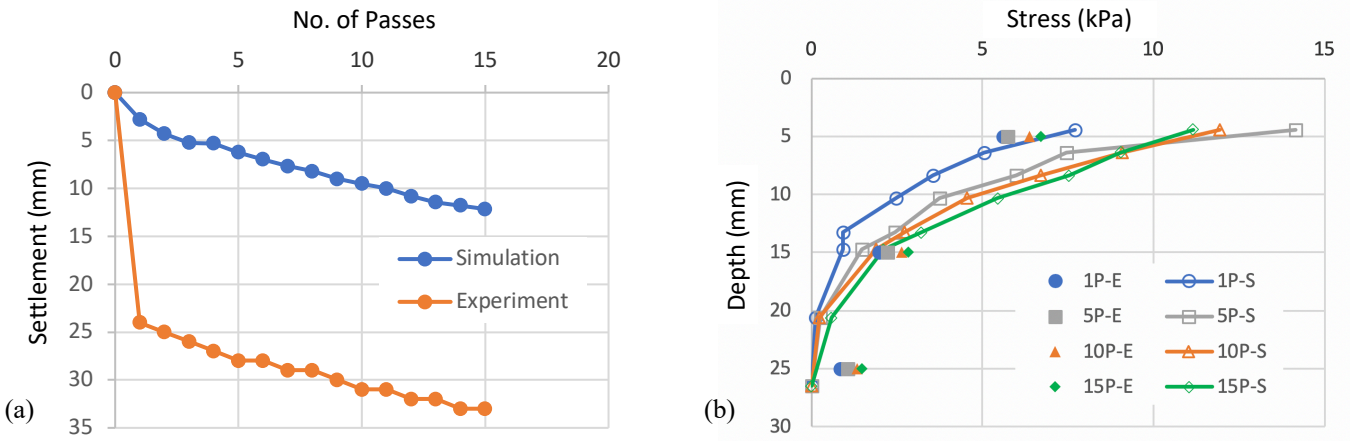

Figure 20: ABAQUS results: (a) surface settlement, (b) stress distribution.
(Legend: 1P-E = Pass 1–experimental, 1P-S = Pass 1–simulation)

6. Artificial Intelligence

In an effort to develop robust predictive models to forecast the performance of RDC, the artificial intelligence (AI) techniques of artificial neural networks (ANNs) and genetic programming (GP), which have already been proven to be successful in a wide variety of forecasting applications in geotechnical engineering, have been examined. The AI-based models incorporate comprehensive databases consisting of in situ soil test data; in particular, cone penetration test (CPT) and dynamic cone penetration (DCP) test data obtained from past ground improvement projects involving the BH-1300, 8-tonne, 4-sided impact roller. Altogether, four predictive models have been developed: two based on ANNs – one for the CPT and the other for the DCP; and two GP models – again, one for the CPT and the other for the DCP. These models are briefly discussed below.

6.1. Artificial Neural Networks

ANNs can be considered as the most widely used AI technique [41], by which its architecture attempts to simulate the functionality of the human brain and neuron system [42]. ANNs learn from previous examples and obtain knowledge from data and, as such, the functional relationships among variables are captured when they are presented with a set of inputs and their corresponding outputs.

The AI models developed in this study, predict the improvement in in situ density of the ground at depth as a result of RDC. As such, the models with CPT data predict the degree of density improvement of the ground in terms of the cone tip resistance, q_{cf} (MPa), after certain number of roller passes. Similarly, the AI models with DCP data incorporate a single output variable expressing the average DCP blow count per 300 mm, by which the degree of density improvement with respect to a certain number of roller passes is indirectly quantified. In predicting these, the models are presented with a comprehensive set of input variables that addresses the key factors affecting ground density improvement by means of RDC. As such, the CPT data-based AI models employ 4 input variables: depth, D (m); cone tip resistance prior to compaction, q_{ci} (MPa); sleeve friction prior to compaction, f_{si} (kPa); and the number of roller passes, P. The AI models incorporating DCP data consist of 5 input variables: soil type; average depth, D (m); initial number of roller passes, P_i; initial DCP count (blows/300 mm); and the final number of roller passes, P_f.

The resulting optimal ANN-based models were found to be capable of predicting the target values to a high degree of accuracy, with a high coefficient of correlation (R > 0.8) and with low prediction error values, i.e. root mean square error (RMSE) and mean absolute error (MAE), when validated against a set of unseen data. The performance statistics are presented in Table 2. As can be seen, there exists very good correlation between the model predictions and the measured values, by which it is confirmed that the developed ANN models provide accurate predictive capabilities.

Table 2: Performance statistics of the optimal ANN models.

AI Model–Data type	R	RMSE	MAE
ANN–CPT	0.86	4.16	2.93
ANN–DCP	0.79	7.54	5.59

Note: For CPT models, units are MPa and for DCP models, units are blows/300 mm.

6.2. Genetic Programming

The other AI approach which is adopted in the present study, GP, makes use of the principle of Darwinian natural evolution [43] and mimics the aspects of genetics and natural selection. In comparison, GP and its variants can be considered as fairly novel among other modelling approaches of prediction and forecasting problems [44]. However, in recent years, GP has emerged to be a promising approach for non-linear modelling of different aspects in the field of geotechnical engineering.

As with the ANN models discussed above, the GP models were found to be effective when predicting the density development of the ground with respect to the number of impact roller passes and the associated subsurface conditions. The model predictions were found to be accurate, as evidenced by the high correlation coefficients and relatively lower error values, when validated against a set of unseen data, as presented the optimal results in Table 3.

Table 3: Performance statistics of the optimal GP models.

AI Model–Data type	R	RMSE	MAE
GP–CPT	0.87	4.03	2.71
GP–DCP	0.81	6.80	4.74

Note: For CPT models, units are MPa and for DCP models, units are blows/300 mm.

Both the ANN- and GP-based optimal models were examined further by using several other means including analysing the geotechnical property distributions and examining various parametric studies to assess the generalisation ability and the robustness of the models. In addition, a comparative study was conducted, where the performance of the optimal ANN- and GP-based models were compared with one another with the intention of selecting the most feasible approach for predicting the effectiveness of RDC in different ground conditions with respect to CPT and DCP test data. As such, it has been demonstrated that the GP-based models slightly outperform their ANN counterparts and overall produce slightly more accurate predictions. Additionally, the optimal model behaviour was examined in presence of new datasets. For example, the capabilities of both the optimal ANN and GP models are further evaluated and compared by introducing, to the models,

a series of unseen complete CPT datasets randomly chosen from the RDC projects. As can be seen from Figure 21, the model predictions were found to align strongly with the measured data.

It is evident that both the ANN- and GP-based models developed in this study are successful in providing reliable predictions of the effectiveness of RDC in various ground conditions. As such, it has been shown that the application of both ANNs and GP in relation to RDC is entirely appropriate and useful, given that no other predictive tools, conventional or AI-based, are available. Moreover, it is recommended that the developed models are valuable for the estimations needed during the pre-planning and pre-design phases of ground improvement projects involving RDC. Details of the ANN–CPT, ANN–DCP, GP–CPT and GP–DCP models are given by [45–48] respectively.

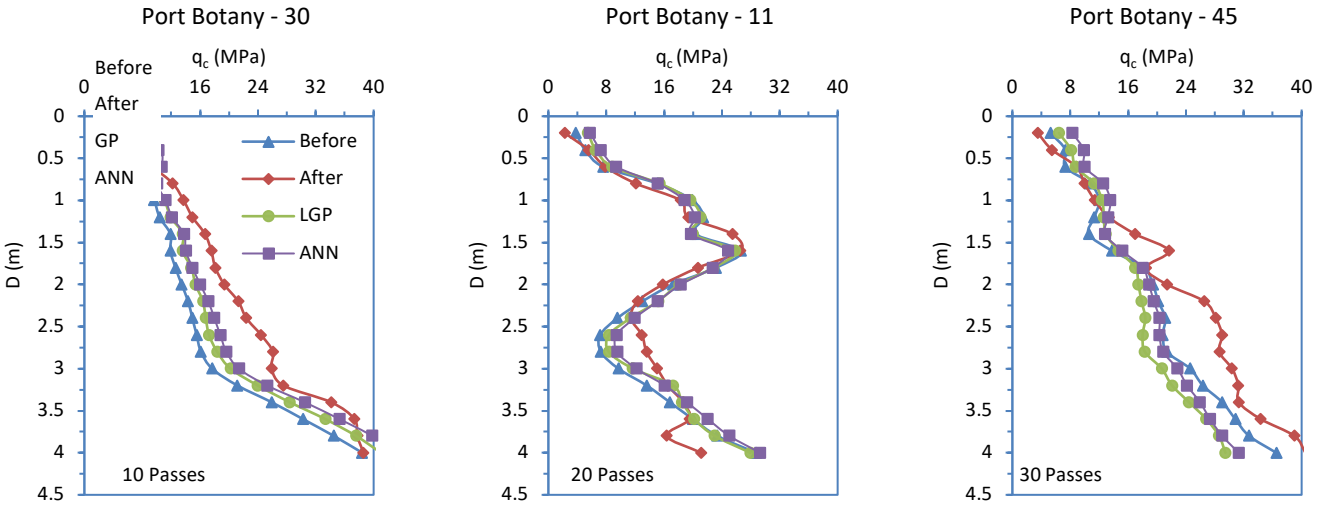

Fig. 21: Plots of actual and AI-based model predicted CPT results.

7. Transparent Soils

In an effort to understand better the mechanics of RDC and its compactive effect, transparent soils are being examined. Transparent soil is a two-phase medium, which consists of solid, transparent surrogates and a matched refractive index pore fluid [49]. The use of transparent soil significantly improves the visualisation of soil movement within a soil mass and facilitates the assessment of particle displacement. Fused quartz (Fig. 22) is being used as the soil surrogate as it is stable and hard; its angularity is similar to that of sand; and it exhibits high transparency. Sodium-thiosulfate treated sodium-iodide solution (STSI) is being used as the matched refractive index pore fluid to form the transparent soil. The main advantages of STSI are: the viscosity of STSI is comparable to water; STSI is a water-based solution, therefore, it is more representative of geoenvironmental applications; and STSI can be recycled and reused in multiple tests, making it a more environmentally-friendly and cost-effective material. Figure 23 shows text printed on a sheet of white paper which is placed behind a 60 mm thickness of fused quartz with no pore fluid (Fig. 23a) and after the addition of STSI pore fluid (Fig. 23b). It can be clearly observed that the addition of the STSI pore fluid dramatically improves the transparency of the fused quartz.

The transparent soil is currently being used at the Broons-University of Adelaide physical model test facility (Fig. 7) to examine, in the first instance, the nature of ground improvement due to the 4-sided roller. This research endeavour is in its very early stages. Soil particle displacement will be investigated using a bespoke laser arrangement, which will illuminate a cross-sectional plane of soil immediately beneath the centreline of the roller and create a speckled pattern which, when used in conjunction with the digital image correlation (DIC) method [50] and a high-resolution camera, will enable soil particle motion beneath the RDC module to be examined. This will facilitate the study of the relative displacements of the particles, the evolution of soil density and, hence, ground improvement.

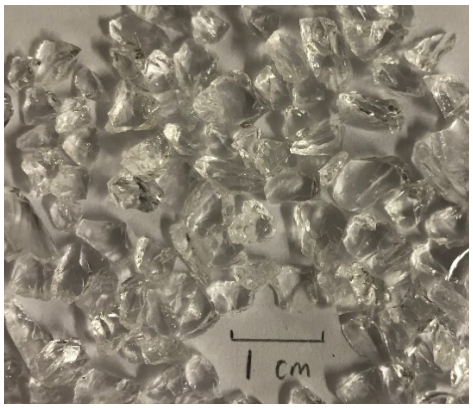

Fig. 22: Fused quartz.

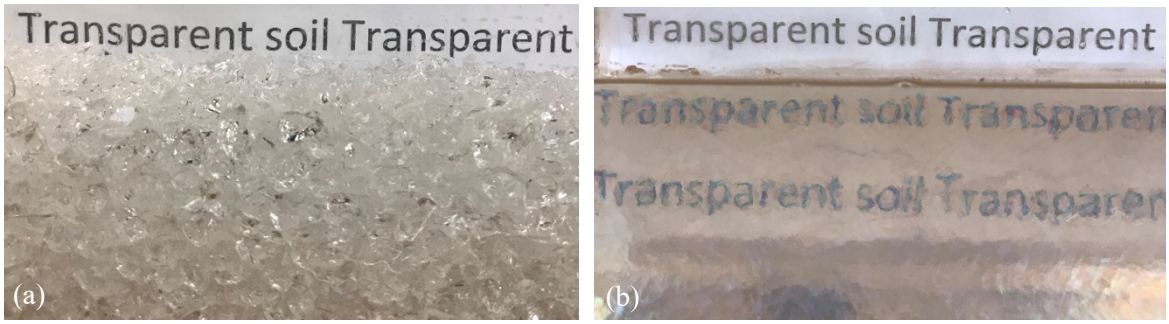

Fig. 23: Transparent soil with text viewed from behind a 60 mm thickness of fused quartz with: (a) no pore fluid, (b) STSI pore fluid.

8. Conclusions

This paper has presented a relatively brief overview of a broad and comprehensive research program currently being undertaken at the Universities of Adelaide and Sydney to study the behaviour and influence of rolling dynamic compaction (RDC). This technology is increasingly adopted throughout the world because of its effectiveness and efficiency and research is needed to better understand and characterise its behaviour and its effectiveness. To date, the research program has involved a mix of field and laboratory testing and numerical modelling. These research endeavours have demonstrated that RDC is indeed an effective means of ground improvement and that it is more efficient and improves the ground to greater depths than traditional means of surface compaction.

Acknowledgements

Such a large research effort can only be undertaken with the assistance of a committed group of capable and enthusiastic individuals. Firstly, the authors are grateful to the Director of Broons, Mr. Stuart Bowes, for his continued support of this research effort. Without his support, generosity and counsel, this research would not be possible. Thanks are also due to Derek Avalle, from Broons, for his ongoing engagement, enthusiasm and advice. A number of final-year, undergraduate civil engineering students, at the Universities of Adelaide and Sydney, as well as Masters students, have contributed greatly to this work. These include: T. Balomenos, T. Bierbaum, S. Brown, G. Canala, B. Chau, G. Chen, Z. Chen, S. Chenoweth, J. Colbert, A. Crisp, Z. Deng, C. Gauro, M. Haywood, J. Jiang, A. Kamarrudin, C.T. Lai, R. Lane, D. Liu, Y. Lou, V. Lucas, J. March, M. Masoudian, N. Mentha, T. Muecke, D. Nguyen, S. O'Dea, G. Peters, S. Phommala, J. Piotto, S. Pointon, C. Power, P. Rajarathnam, J. Saw, T. Schwarz, A. Sedgley, C. Smith, K. Steele, R. Strapps, E. Syamsuddin, S. Syed Abdul Aziz, A. Symons, T. Treloar, R. Vince, T. Vo, S. Whalley, P. Wrightson, Y. Yan, S. Yang, Z. Yu. In addition, this work would not have been possible for the important and significant technical support received from Gary Bowman, Ian Cates, Terry Cox, Simon Golding, Tom Stanef and Stan Woithe (University of Adelaide), and Ross Barker and Sergio de Carvahlo (University of Sydney). The authors are truly grateful for their efforts. Finally, but by no means least, the authors wish to thank the Australian Research Council for providing significant funding to realise the research objectives.

References

[1] J. M. Clifford, "Impact rolling and construction techniques," in *Proceedings of the 8th Conference of the Australian Road Research Board,* Perth, Australia, 1976, vol. 8, pp. 21–29.

[2] D. L. Avalle, "Ground improvement using the 'square' impact roller – case studies," in *Proceedings of the 5th International Conference on Ground Improvement Techniques*, Kuala Lumpur, Malaysia, 2004, pp. 101–108.

[3] I. Jumo and J. Geldenhuys, "Impact compaction of subgrades-experience on the Trans-Kalahari Highway including continuous impact response (CIR) as a method of quality control," in *Proceedings of the 8th Conference on Asphalt Pavements for Southern Africa*, Sun City, South Africa, 2004, paper 19.

[4] D. L. Avalle, "Use of the impact roller to reduce agricultural water loss," in *Proceedings of the 9th Australia New Zealand Conference on Geomechanics*, Auckland, New Zealand, 2004, pp. 513–518.

[5] M. I. Pinard, "Innovative developments in compaction technology using high energy impact compactors," in *Proceedings of the 8th Australia New Zealand Conference on Geomechanics*, Hobart, Australia, 1999, vol. 2, pp. 775–781.

[6] B.T. Scott, M. B. Jaksa and Y. L. Kuo, "Use of Proctor compaction testing for deep fill construction using impact rollers," in *Proceedings of the International Conference on Ground Improvement and Ground Control*, Wollongong, Australia, 2012, pp. 1107–1112.

[7] B. T. Scott and M. B. Jaksa, "The effectiveness of rolling dynamic compaction–a field based study," in *Ground Improvement Case Histories: Compaction, Grouting and Geosynthetics,* B. Indraratna, J. Chu and C. Rujikiatkamjorn, Eds. Kidlington, Oxford: Elsevier, 2015, pp. 429–452.

[8] B. T. Scott and M. B. Jaksa, "Quantifying the influence of rolling dynamic compaction," in *Proceedings of the 8th Young Geotechnical Professionals Conference,* Wellington, New Zealand, 2008, pp. 199–204.

[9] Geokon, "Instruction Manual Model 3500, 3510, 3515, 3600 Earth Pressure Cells." Geokon Incorporated, Lebanon, USA, 2007.

[10] D. L. Avalle, B. T. Scott, and M. B. Jaksa, "Ground energy and impact of rolling dynamic compaction—results from research test site," in *Proceedings of the 17th International Conference on Soil Mechanics and Geotechnical Engineering,* Alexandria, Egypt, 2009, vol. 3, pp. 2228–2231.

[11] National Instruments. (2018, December 7). [Online]. Available: http://www.ni.com/manuals/

[12] B. T. Scott, M. B. Jaksa and E. Syamsuddin, "Verification of an impact rolling compaction trial using various in situ testing methods," in *Proceedings of the 5th International Conference on Geotechnical and Geophysical Site Characterisation,* Gold Coast, Australia, 2016, pp. 735–740.

[13] B. T. Scott, M. B. Jaksa and P. W. Mitchell, "Depth of influence of rolling dynamic compaction," in *Proc. of ICE – Ground Improvement*, 2019.

[14] H. K. W. Wong and J. C. Small, "Effect of orientation of approach slabs on pavement deformation," *J. Transp. Eng.*, vol. 120, no. 4, pp. 590–602, 1994.

[15] F. Moghaddas-Nejad and J. C. Small, "Effect of geogrid reinforcement in model track tests on pavements," *J. Transp. Eng.*, vol. 127, no. 6, pp. 468–474, 1996.

[16] Z. Yu, "Investigating the effects of rolling dynamic compaction using a reduced-size model," B.Eng. Thesis, Dept. Civil Eng., Uni. of Sydney, Sydney, Australia, 2014.

[17] P. Rajarathnam, "Dynamic effects in soil – dynamic compaction," M.Eng. Thesis, Dept. Civil Eng., Uni. of Sydney, Sydney, Australia, 2015.

[18] C. Wersall, S. Larsson, N. Ryden and I. Nordfelt, "Frequency variable surface compaction of sand using rotating mass oscillators," *Geotech. Testing J.*, vol. 38, no. 2, pp. 198–207, 2015.

[19] D. L. Avalle, "A note on specifications for the use of the impact roller for earthworks," in *Proceedings of the Earthworks Seminar*, Adelaide, Australian Geomechanics Society, 2004.

[20] D. L. Avalle, "Impact rolling in the spectrum of compaction techniques and equipment," in *Proceedings of the Earthworks Seminar*, Adelaide, Australian Geomechanics Society, 2004.

[21] O. Y. Chung, B. Scott, M. Jaksa, Y. L. Kuo and D. Airey, "Physical modelling of rolling dynamic compaction," in *Proceedings of the 19th International Conference on Soil Mechanics and Geotechnical Engineering*, Seoul, Korea, pp. 905–908, 2017.

[22] W. D. Hillis, "Active touch sensing," *Artificial Intelligence Laboratory Memo 629*, Massachusetts Institute of Technology, Cambridge, MA, 1981.
[23] J. A. Purbrick, "A force transducer employing conductive silicone rubber," in *Proceedings of First Robotic Vison and Sensors Conference, Stratford-on-Avon*, UK, 1981.
[24] Tekscan Inc. "Calibration for high speed application – Revision B," Tekscan Inc., South Boston, Mass., 2016.
[25] S. G. Paikowsky, E. L. Hajduk, "Calibration use of grid-based tactile pressure sensors in granular material," *Geotech. Testing J.*, vol. 20, no. 2, pp. 218–241, 1997.
[26] S. M. Springman, P. Nater, R. Chikatamarla and J. Laue, "Use of flexible tactile pressure sensors in geotechnical centrifuge," in *Proceedings of the International Conference of Physical Modeling in Geotechnical Engineering*, St. John's, Canada, 2002, pp. 113–118.
[27] S. G. Paikowsky, C. J. Palmer and L. E. Rowles, "The use of tactile sensor technology for measuring soil stress distribution," in *Proceedings of GeoCongress 2006: Geotechnical Engineering in the Information Technology Age*, ASCE, Atlanta, Georgia, 2006, pp. 1–6.
[28] M. C. Palmer, T. D. O'Rourke, N. A. Olson, T. Abdoun, D. Ha and M. J. O'Rourke, "Tactile pressure sensors for soil-structure interaction assessment," *J. Geotech. and Geoenv. Engrg.*, vol. 135, no. 11, pp. 1638–1645, 2009.
[29] Shining 3D. (2018, November 29). "Einscan Pro +" [Online]. Available: https://www.einscan.com/einscan-pro-plus
[30] B. Bastaee and M. Parvizi, "Experimental and numerical analysis of impact roller on clay overlaying sand," in *Proceedings of the 15th International Conference on Experimental Mechanics*, Porto, Portugal, 2012, paper 2627.
[31] K. Kim, *Impact Rollers (Soil Compaction) Numerical Simulation of Impact Rollers for Estimating the Influence Depth of Soil Compaction.* Saarbrucken: LAP Lambert Academic Publishing, 2011.
[32] A. B. Bradley, A. C. Crisp, J. H. Jiang, and C. N. Power, "Assessing the effectiveness of rolling dynamic compaction using LS-DYNA," BE(Hons.) dissertation, School of Civil, Env. and Mining Engrg., Uni. of Adelaide, Adelaide, Australia, 2012.
[33] Y. L. Kuo, M. B. Jaksa, B. T. Scott, A. C. Bradley, C. N. Power, A. C. Crisp and J. H. Jiang, "Assessing the effectiveness of rolling dynamic compaction," in *Proceedings of the 18th International Conference on Soil Mechanics and Geotechnical Engineering*, Paris, France, 2013, pp. 1309–1312.
[34] E. Nohani and H. Mirzaei, "Distribution of effective stress in compaction of earth dams due to the three-sided impact roller and comparing with four-sided roller field data," *Int. J. Res. and Reviews in Appl. Sc.*, vol. 21, no. 3, pp. 114–124, 2014.
[35] J. M. Clifford and G. Bowes, "Calculating the energy delivered by an impact roller: A trilogy of papers for the Sept. 1995 lecture tour and int. seminars to commemorate the 10th anniversary of the BH-1300 impact roller," paper 2, 1995, pp. 1–15.
[36] A. C. Bradley, M. B. Jaksa, Y. L. Kuo and T. Bennett, "A finite element model for heavy tamping on dry sand," in *Proceedings of the 16th European Conference on Soil Mechanics and Geotechnical Engineering*, Edinburgh, UK, 2015, pp. 1377–1382.
[37] Q. Gu and F. H. Lee, "Ground response to dynamic compaction of dry sand," *Géotechnique*, vol. 52, no. 7, pp. 481–493, 2002.
[38] T. Belytschko and L. P. Binderman, "Assumed strain stabilization of the eight node hexahedral element," *Computer Methods in Appl. Mech. and Engrg.*, vol. 105, no. 2, pp. 225–226, 1993.
[39] Z.-Q. Chen, C. Xu and Y. Lü, "Model test of impact roller compaction for dry sand," *Rock and Soil Mech.*, vol. 36, no. 2, pp. 525–531, 2015. (in Chinese).
[40] P. Rajarathnam, M. S. Masoudian, M. Jaksa and D. W. Airey, "Model tests of rolling dynamic compaction," in *Proceedings of the 19th Southeast Asian Geotechnical Conference*, Kuala Lumpur, Malaysia, 2016, pp. 505–510.
[41] P. Aminian, H. Niroomand, A. Hossein Gandomi, A. Hossein Alavi and M. Arab Esmaeili, "New design equations for assessment of load carrying capacity of castellated steel beams: a machine learning approach," *Neural Computing and Appl.*, vol. 23, no. 1, pp. 119–131, 2013.
[42] M. A. Shahin, M. B. Jaksa and H. R. Maier, "State of the art of artificial neural networks in geotechnical engineering," *Electronic J. Geotech. Engrg.*, vol. 2008, no. 8, pp. 1–26, 2008.
[43] J. R. Koza, *Genetic Programming: On the Programming of Computers by Means of Natural Selection*. Vol. 1, MIT Press USA, 1992.

[44] A. Hossein Alavi, A. Hossein Gandomi, A. Mollahasani and J. Bolouri Bazaz, "Linear and tree-based genetic programming for solving geotechnical engineering problems," in *Metaheuristics in Water, Geotechnical and Transport Engineering*, X.-S. Yang, A. Hossein Gandomi, S. Talatahari and A. Hossein Alavi, Eds. London: Elsevier, 2013, pp. 289–310.
[45] R. A. T. M. Ranasinghe, M. B. Jaksa, Y. L. Kuo and F. Pooya Nejad, "Prediction of the effectiveness of rolling dynamic compaction using artificial neural networks and cone penetration test data," *Chinese J. of Rock Mech. and Engrg.*, vol. 38, no. 1, pp. 153–170, 2019.
[46] R. A. T. M. Ranasinghe, M. B. Jaksa, Y. L. Kuo and F. Pooya Nejad, "Application of artificial neural networks for predicting the impact of rolling dynamic compaction using dynamic cone penetrometer test results," *J. of Rock Mech. and Geotech. Engrg.*, vol. 9, no. 2, pp. 340–349, 2017.
[47] R. A. T. M. Ranasinghe, M. B. Jaksa, Y. L. Kuo and F. Pooya Nejad, "Predicting the Effectiveness of Rolling Dynamic Compaction Using Genetic Programming and Cone Penetration Test Data," in *Proc. of Inst. of Civil Engineers – Ground Improvement*, vol. 170, no. 4, pp. 193–207, 2017.
[48] R. A. T. M. Ranasinghe, M. B. Jaksa, Y. L. Kuo and F. Pooya Nejad, "Use of Genetic programming for the predictions of effectiveness of rolling dynamic compaction using dynamic cone penetrometer test results," *J. of Rock Mech. and Geotech. Engrg.*, 2019.
[49] M. Iskander, R. Bathurst and M. Omidvar, "Past, present, and future of transparent soils," *Geotech. Testing J.*, vol. 38, no. 5, pp. 557–573, 2015.
[50] H. Horii, K. Takamatsu, J. Inoue and N. Sasaki, "Measurement of displacement field by matching method and observation of strain localization in soft rock," in *Proceedings of the 2nd International Conference on Imaging Technologies: Techniques and Applications in Civil Engineering*, Davos, Switzerland, 1997, pp. 10–19.